Journal of Porphyrins and Phthalocyanines
J. Porphyrins Phthalocyanines 2014; **18**: 1–14
DOI: 10.1142/S1088424614501107

Published at http://www.worldscinet.com/jpp/

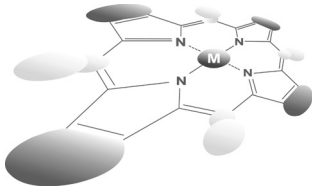

Design of diethynyl porphyrin derivatives with high near infrared fluorescence quantum yields

Kimihiro Susumu[a,c,d] **and Michael J. Therien***[b◊]

[a] *Department of Chemistry, 231 South 34th Street, University of Pennsylvania, Philadelphia, PA 19104-6323, USA*
[b] *Department of Chemistry, French Family Science Center, 124 Science Drive, Duke University, Durham, NC 27708-0346, USA*

Dedicated to Professor Shunichi Fukuzumi on the occasion of his retirement

Received 6 October 2014
Accepted 11 November 2014

ABSTRACT: A design strategy for (porphinato)zinc-based fluorophores that possess large near infrared fluorescence quantum yields is described. These fluorophores are based on a (5,15-diethynylporphinato) zinc(II) framework and feature symmetric donor or acceptor units appended at the *meso*-ethynyl positions *via* benzo[c][1,2,5]thiadiazole moieties. These (5,15-bis(benzo[c][1′,2′,5′]thiadiazol-4′-ylethynyl)-10,20-bis[2′,6′-bis(3″,3″-dimethyl-1″-butyloxy)phenyl]porphinato)zinc(II) (**4**), (5,15-bis[4′-(*N*,*N*-dihexylamino) benzo[c][1′,2′,5′]thiadiazol-7′-ylethynyl]-10,20-bis[2′,6′-bis(3″,3″-dimethyl-1″-butyloxy)phenyl] porphinato)zinc(II) (**5**), (5,15-bis([7′-(4″-*n*-dodecyloxyphenylethynyl)benzo[c][1′,2′,5′]thiadiazol-4′-yl] ethynyl)-10,20-bis[2′,6′-bis(3″,3″-dimethyl-1″-butyloxy)phenyl]porphinato)zinc(II) (**6**), (5,15-bis([7′-([7″-(4‴-*n*-dodecyloxyphenyl)benzo[c][1″,2″,5″]thiadiazol-4″-yl]ethynyl)benzo[c][1′,2′,5′]thiadiazol-4′-yl]ethynyl)-10,20-bis[2′,6′-bis(3″,3″-dimethyl-1″-butyloxy)phenyl]porphinato)zinc(II) (**7**), 5,15-bis ([7′-(4″-*N*,*N*-dihexylaminophenylethynyl)benzo[c][1′,2′,5′]thiadiazol-4′-yl]ethynyl)-10,20-bis[2′,6′-bis(3″,3″-dimethyl-1″-butyloxy)phenyl]porphinato)zinc(II) (**8**), and (5,15-bis([7′-(4″-*N*,*N*-dihexylaminophenylethenyl)benzo[c][1′,2′,5′]thiadiazol-4′-yl]ethynyl)-10,20-bis[2′,6′-bis(3″,3″-dimethyl-1″-butyloxy)phenyl]porphinato)zinc(II) (**9**) chromophores possess red-shifted absorption and emission bands that range between 650 and 750 nm that bear distinct similarities to those of the chlorophylls and structurally related molecules. Interestingly, the measured radiative decay rate constants for these emitters track with the integrated oscillator strengths of their respective x-polarized Q-band absorptions, and thus define an unusual family of high quantum yield near infrared fluorophores in which emission intensity is governed by a simple Strickler–Berg dependence.

KEYWORDS: diethynylporphyrin, benzo[c][1,2,5]thiadiazole, near infrared, fluorescence quantum yield, Strickler–Berg.

INTRODUCTION

The design and synthesis of near infrared (NIR) absorption materials that possess large absorptive oscillator strengths and high fluorescence quantum yields are important to molecular imaging [1–5] and solar energy conversion technologies [6–10]. Likewise, the efficient utilization of NIR sunlight is a key feature of natural photosynthesis, which exploits NIR-absorbing dyes such as chlorophylls and pheophytins [11]. Relative to the tremendous attention that has been paid to the design and synthesis of low band gap chromophores and materials [12–19], much less focus has been given to the development of strategies that channel enhanced oscillator strength into the low energy optical transitions

◊SPP full member in good standing

*Correspondence to: Michael J. Therien, tel: +1 919-660-1670, email: michael.therien@duke.edu
Current address: [c]Optical Sciences Division, U.S. Naval Research Laboratory, Washington, DC 20375, USA; [d]Sotera Defense Solutions, Inc., Columbia, MD 21046, USA

of such compositions. For example, only a limited number of conjugated organic structures possess both high oscillator strength NIR ($S_0 \rightarrow S_1$) absorptions and corresponding high ($S_1 \rightarrow S_0$) fluorescence quantum yields [20, 21]. In general, a higher $S_0 \rightarrow S_1$ absorptive extinction coefficient should correlate with a larger $S_1 \rightarrow S_0$ radiative rate constant, congruent with the Strickler–Berg relationship [22]; most strongly absorbing organic NIR dyes, however, are not impressive emitters, due in many cases to large magnitude S_1 state non-radiative rate constants that are readily rationalized within the context of the energy gap law [23].

Porphyrins are tetrapyrrole π-conjugated systems, and the lowest energy absorption bands of simple tetraphenylporphyrin or octaethylporphyrin monomers range typically over the 600 to 650 nm spectral regime and feature modest absorptive extinction coefficients ($\varepsilon < 10^4\ M^{-1}.cm^{-1}$). Modification of the porphyrin π-skeleton can further reduce the HOMO–LUMO gap; the electronic structures of such reduced band gap porphyrins can in general be rationalized using Gouterman's four orbital model [24]. In a simple (porphinato)metal complex having D_{4h} symmetry, the LUMO is doubly degenerate, and the HOMO and HOMO-1 are nearly degenerate in energy; as a result, substantial configuration interaction mixes the ($a_{1u} \rightarrow e_g$) and ($a_{2u} \rightarrow e_g$) transitions. Constructive and destructive combinations of these one-electron transitions give rise to an intense shorter-wavelength Soret band and a weakly absorbing longer-wavelength Q-band. While removal of frontier orbital (HOMO/HOMO-1, LUMO/LUMO+1) degeneracy is expected to result in augmentation of the Q-band absorptive extinction coefficient, relatively few examples exist of low band gap porphyrin derivatives that possess intense NIR Q-bands [25–29].

In contrast, the chlorophylls, natural porphyrin derivatives, possess lowest energy Q-bands with significant extinction coefficients (ε: $0.5 \sim 1 \times 10^5\ M^{-1}.cm^{-1}$) [30, 31]; some chlorophyll derivatives and related macrocycles feature substantial fluorescence quantum yields that range from ~0.05 to 0.3 [32, 33]. While significant strides have been made in recent years regarding chlorophyll synthesis [33–35], the more involved nature of their fabrication limits many possible applications of these structures. Chromophores within the phthalocyanine family also exhibit intense low energy electronic absorption bands (ε: $1 \sim 2 \times 10^5\ M^{-1}.cm^{-1}$); while a few examples of these chromophores are known that feature both substantial NIR absorptivity and significant fluorescence quantum yield (0.1 ~ 0.8) [36, 37], it is important to point out that extensive modulation of phthalocyanine absorptive properties and photophysics is limited by the modest frontier orbital electron density localized at the periphery of the macrocycle-fused benzene rings [38].

We have explored synthesis and electronic properties of *meso*-ethynyl porphyrin derivatives [39–62] for nonlinear optics [60, 63–81], optoelectronic devices [82–87], and fluorescence-based optical imaging technologies [88–97]. Ethyne groups fused to the porphyrin *meso*-positions provide significant electronic interaction with the macrocycle a_{2u}-derived HOMO and remove the degeneracy of the low-lying empty e_g orbitals [39, 42, 45, 50, 55]. Here we report the synthesis and optical properties of conjugated 5,15-diethynyl(porphinato)zinc(II) complexes that feature conjugated terminal groups having varying degrees of proquinoidal character (Fig. 1) that drive intense Q-band absorptions; the uncommon emissive properties of these new fluorophores based on a (5,15-diethynylporphinato) zinc(II) framework are discussed within the context of the Strickler–Berg relationship.

EXPERIMENTAL

Materials

All manipulations were carried out under nitrogen previously passed through an O_2 scrubbing tower (Schweitzerhall R3-11 catalyst) and a drying tower (Linde 3-Å molecular sieves) unless otherwise stated. Air sensitive solids were handled in a Braun 150-M glove box. Standard Schlenk techniques were employed to manipulate air-sensitive solutions. Tetrahydrofuran (THF) was distilled from K/4-benzoylbiphenyl under N_2. Triethylamine and MeOH were distilled from CaH_2 under N_2. The catalysts $Pd(PPh_3)_4$, $Pd(PPh_3)_2Cl_2$, dichloro[1,1′-bis(diphenylphosphino)ferrocene]palladium(II) dichloromethane adduct, P(*t*-Bu)$_3$ (10 wt% solution in hexanes), tris(dibenzylideneacetone)dipalladium(0) (Pd_2dba_3), CuI and triphenylarsine ($AsPh_3$) were purchased from Strem Chemicals and used as received. 4-Bromobenzo[c][1,2,5]thiadiazole, and 4,7-dibromobenzo[c][1,2,5]thiadiazole were prepared by literature methods [98]. (5,15-Bis[trimethylsilylethynyl]-10,20-bis[3′,5′-bis(9″-methoxy-1″,4″,7″-trioxanonyl)phenyl]porphinato)zinc(II) (**1**), (5,15-dibromo-10,20-bis[2′,6′-bis(3″,3″-dimethyl-1″-butyloxy)phenyl] porphinato)zinc(II), (5,15-diethynyl-10,20-bis[2′,6′-bis(3″,3″-dimethyl-1″-butyloxy)phenyl]porphinato)zinc(II), and (5,15-bis(4′-(*N*,*N*-dimethylamino)phenylethynyl)-10,20-bis[2′,6′-bis(3″,3″-dimethyl-1″-butyloxy)phenyl]porphinato)zinc(II) (**2**) were synthesized as described previously [50, 54, 66]. A number of key precursors were synthesized as reported earlier [99]. All NMR solvents, and all other chemicals, were used as received.

Chemical shifts for ^{1}H NMR spectra are relative to the tetramethylsilane (TMS) signal in deuterated solvent (TMS, $\delta = 0.00$ ppm). All *J* values are reported in Hertz. Flash and size exclusion column chromatography were performed on the bench top, using respectively silica gel (EM Science, 230–400 mesh) and Bio-Rad Bio-Beads SX-1 as media. CI mass spectra were acquired at the Mass Spectrometry Center at the University of Pennsylvania. MALDI-TOF mass spectroscopic data were obtained with a Voyager-DE RP instrument

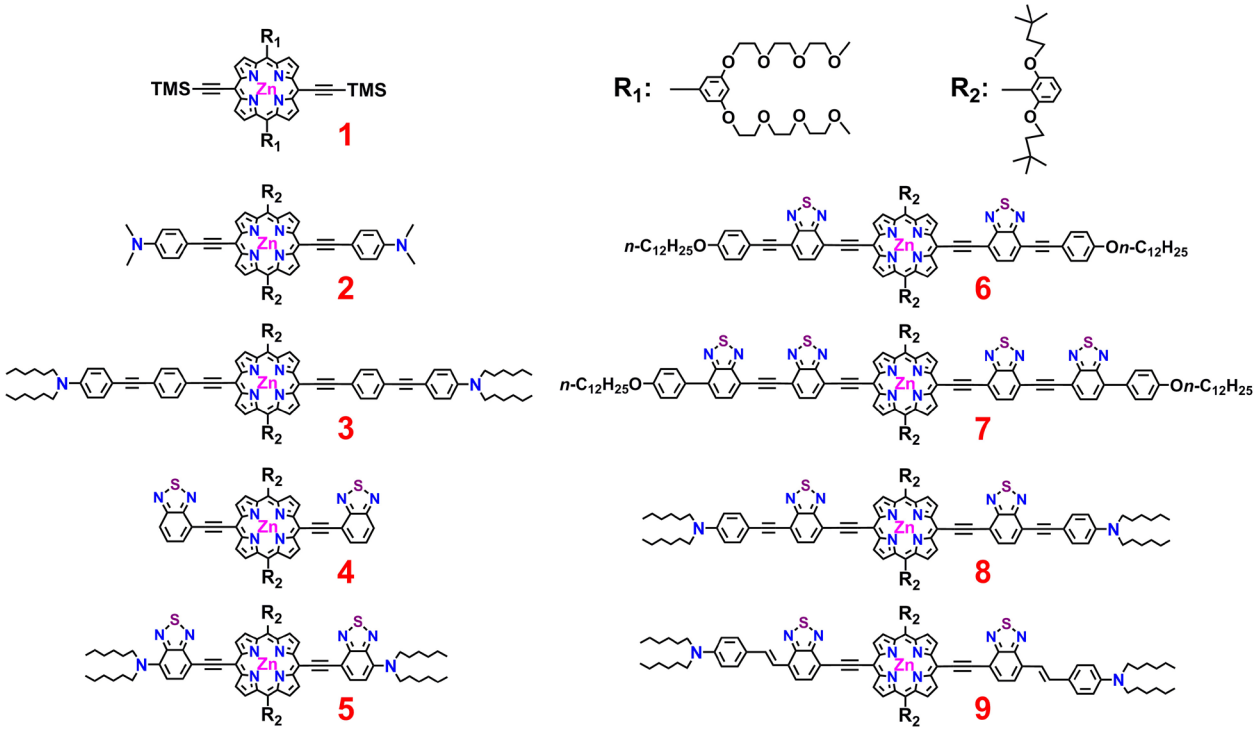

Fig. 1. Structures of the TMS-protected (5,15-diethynyl-10,20-bis[3′,5′-bis(9″-methoxy-1″,4″,7″-trioxanonyl)phenyl]porphinato) zinc(II) reference monomer (**1**), and NIR fluorophores **2–9**

(PerSeptive Biosystems); samples for these experiments were prepared as micromolar solutions in either CH_2Cl_2 or THF, and dithranol (Sigma–Aldrich) was utilized as the matrix.

Instrumentation

^{1}H NMR spectra were recorded on either 250 MHz AC-250, 300 MHz DMX-300, or 500 MHz AMX-500 Brüker spectrometers. Electronic absorption spectra were recorded on a Shimadzu PharmaSpec UV1700 spectrophotometer. Fluorescence spectra were obtained with a Spex Fluorolog-3 spectrophotometer (Jobin Yvon Inc., Edison, NJ) that utilized a T-channel configuration with red sensitive R2658 Hamamatsu PMT and liquid nitrogen cooled InGaAs detectors. The obtained fluorescence spectra were corrected using the spectral output of a calibrated light source supplied by the National Bureau of Standards. Fluorescence quantum yields were measured on N_2-purged solutions at room temperature. Tetraphenylporphyrin in benzene (Φ_f = 0.13) was used as a standard [100]. The fluorescence quantum yields of each sample were calculated using the following equation (Equation 1)

$$\frac{\Phi_{f(s)}}{\Phi_{f(r)}} = \frac{F_s \cdot A_r \cdot n_s^2}{F_r \cdot A_s \cdot n_r^2} \quad (1)$$

where Φ_f is the fluorescence quantum yield, F is the area under the corrected fluorescence band (expressed in number of photons), A is the absorbance at the excitation wavelength, and n is the refractive index of the solvents used. Subscripts s and r refer to the sample and reference, respectively. Time-correlated single-photon counting (TCSPC) experiments to measure fluorescence lifetimes were performed using an Edinburgh Analytical Instruments FL/FS 900 spectrofluorimeter. The excitation sources for TCSPC measurements were either a nanosecond flash lamp operating under an atmosphere of H_2 gas (0.50–0.55 bar, 0.7 nm fwhm, 40 kHz repetition rate) or a blue (450 ± 15 nm) light-emitting diode (Picoquant PLS 450/PDL 800-B) triggered at a frequency of 100 kHz by a Berkeley Nucleonics 555 pulse generator. TCSPC data were analyzed by iterative convolution of the fluorescence decay profile with the instrument response function using software provided by Edinburgh Instruments.

Synthesis

(5,15-Bis[4′-(4″-*N*,*N*-dihexylaminophenylethynyl) phenylethynyl]-10,20-bis[2′,6′-bis(3″,3″-dimethyl-1″-butyloxy)phenyl]porphinato)zinc(II) (3). 1-(4′-*N*, *N*-dihexylaminophenylethynyl)-4-iodobenzene [99] (55.5 mg, 1.14×10^{-4} mol), (5,15-diethynyl-10,20-bis[2′,6′-bis(3″,3″-dimethyl-1″-butyloxy)phenyl]porphinato) zinc(II) (50.4 mg, 5.17×10^{-5} mol), $Pd(PPh_3)_4$ (13.2 mg, 1.14×10^{-5} mol), CuI (1.0 mg, 5.3×10^{-6} mol) and dry THF (7.0 mL) were added to a 100-mL round-bottom flask. Ar was bubbled into the reaction mixture for 5 min before

piperidine (0.50 mL) was added. The reaction mixture was stirred at 45 °C for 3.5 h under Ar. After the solvent was evaporated, the residue was chromatographed on silica gel with 8:1 hexanes:THF as the eluent. Yield 0.063 g (72% based on 50.4 mg of (5,15-diethynyl-10,20-bis[2′,6′-bis(3″,3″-dimethyl-1″-butyloxy)phenyl] porphinato)zinc(II)). ^{1}H NMR (300 MHz; $CDCl_3$): δ, ppm 9.67 (d, 4H, J = 4.6 Hz, β-H), 8.86 (d, 4H, J = 4.6 Hz, β-H), 7.96 (d, 4H, J = 8.4 Hz, Ph-H), 7.72 (t, 2H, J = 8.4 Hz, Ph-H), 7.65 (d, 4H, J = 8.4 Hz, Ph-H), 7.43 (d, 4H, J = 8.8 Hz, Ph-H), 7.02 (d, 4H, J = 8.5 Hz, Ph-H), 6.61 (d, 2H, J = 9.0 Hz, Ph-H), 3.92 (t, 8H, J = 7.3 Hz, –O–CH_2–C), 3.30 (t, 8H, J = 7.6 Hz, –N–CH_2–C), 1.60 (m, 8H, –N–C–CH_2–C), 1.2–1.4 (m, 24H, –CH_2–), 0.92 (t, 8H, J = 6.8 Hz, O–C–CH_2–), 0.89 (t, 12H, J = 7.3 Hz, –CH_3), 0.27 (s, 36H, –C–CH_3). MS (MALDI-TOF): m/z 1690.92 (calcd. for $[M]^+$ 1690.976).

4-(Trimethylsilylethynyl)benzo[c][1,2,5]thiadiazole. 4-Bromobenzo[c][1,2,5]thiadiazole (0.378 g, 1.76×10^{-3} mol), $Pd(PPh_3)_4$ (0.125 g, 1.08×10^{-4} mol), CuI (14 mg, 7.4×10^{-5} mol) and dry THF (20 mL) were added to a 100-mL round-bottom flask. Ar was bubbled into the reaction mixture for 5 min before diisopropylamine (1.0 mL) and (trimethylsilyl)acetylene (1.00 mL, 7.1×10^{-3} mol) were added. The reaction mixture was stirred at 45 °C for 11 h under Ar. After cooling, the solvent was evaporated. The residue was chromatographed on silica gel column with 1:1 hexanes:$CHCl_3$ as the eluent. Yield 0.406 g (99% based on 0.378 g of 4-bromobenzo[c][1,2,5]thiadiazole). ^{1}H NMR (300 MHz; $CDCl_3$): δ, ppm 7.99 (dd, 1H, J = 1.0, 8.8 Hz, Ph-H), 7.77 (dd, 1H, J = 1.0, 7.0 Hz, Ph-H), 7.55 (dd, 1H, J = 7.0, 8.8 Hz, Ph-H), 0.34 (s, 9H, –Si–CH_3). MS (CI): m/z 232.048 (calcd. for $[M]^+$ 232.049).

4-Ethynylbenzo[c][1,2,5]thiadiazole. 4-(Trimethylsilylethynyl)benzo[c][1,2,5]thiadiazole (0.100 g, 4.30×10^{-4} mol), K_2CO_3 (78.6 mg, 5.7×10^{-4} mol), THF (3.0 mL), and MeOH (2.0 mL) were added to a 100-mL round-bottom flask. The reaction mixture was stirred at room temperature for 1.5 h under Ar. The reaction mixture was filtered and the solvent was evaporated. Yield quantitative. ^{1}H NMR (300 MHz; $CDCl_3$): δ, ppm 8.04 (d, 1H, J = 8.8 Hz, Ph-H), 7.81 (d, 1H, J = 6.9 Hz, Ph-H), 7.58 (t, 1H, J = 8.0 Hz, Ph-H), 3.59 (s, 1H, ethynyl-H). MS (CI): m/z 160.009 (calcd. for $[M]^+$ 160.010).

(5,15-Bis(benzo[c][1,2,5]thiadiazol-4-ylethynyl)-10,20-bis[2′,6′-bis(3″,3″-dimethyl-1″-butyloxy) phenyl]-porphinato)zinc(II) (4). 4-Ethynylbenzo[c][1,2,5]thiadiazole (40.0 mg, 2.50×10^{-4} mol), (5,15-dibromo-10,20-bis[2′,6′-bis(3″,3″-dimethyl-1″-butyloxy)phenyl]porphinato)zinc(II) (71.0 mg, 2.50×10^{-4} mol), $Pd(PPh_3)_4$ (22.6 mg, 2.0×10^{-5} mol), CuI (2.0 mg, 1.1×10^{-5} mol) and dry THF (10 mL) were added to a 100-mL round-bottom flask. Ar was bubbled into the reaction mixture for 5 min before piperidine (0.50 mL) was added. The reaction mixture was stirred at 48 °C for 24 h under Ar. After cooling, the solvent was evaporated. The residue was chromatographed on silica gel column with 5:1 hexanes:THF as the eluent. The product was further purified by size exclusion column chromatography (Bio Rad Bio-Beads SX-1 packed in THF, gravity flow). Yield 40.7 mg (50% based on 71.0 mg of (5,15-dibromo-10,20-bis[2′,6′-bis(3″,3″-dimethyl-1″-butyloxy)phenyl]porphinato)zinc(II)). ^{1}H NMR (300 MHz; $CDCl_3$): δ, ppm 9.91 (d, 4H, J = 4.5 Hz, β-H), 8.87 (d, 4H, J = 4.5 Hz, β-H), 8.18 (d, 2H, J = 7.0 Hz, Ph-H), 8.07 (d, 2H, J = 8.8 Hz, Ph-H), 7.76 (dd, 2H, J = 7.0, 8.8 Hz, Ph-H), 7.72 (t, 2H, J = 8.4 Hz, Ph-H), 7.03 (d, 4H, J = 8.4 Hz, Ph-H), 3.92 (t, 8H, J = 7.6 Hz, –O–CH_2–C), 0.83 (t, 8H, J = 7.5 Hz, –O–C–CH_2–C), 0.37 (s, 36H, –C–CH_3). MS (MALDI-TOF): m/z 1240.7 (calcd. for $[M]^+$ 1240.441).

(5,15-Bis[4′-(*N*,*N*-dihexylamino)benzo[c][1′,2′,5′] thiadiazole-7′-ylethynyl]-10,20-bis[2′,6′-bis(3″,3″-dimethyl-1″-butyloxy)phenyl]porphinato)zinc(II) (5). 4-Bromo-7-(*N*,*N*-dihexylamino)benzo[c][1,2,5]thiadiazole [99] (53.8 mg, 1.35×10^{-4} mol), (5,15-diethynyl-10,20-bis[2′,6′-bis(3″,3″-dimethyl-1″-butyloxy)phenyl] porphinato)zinc(II) (41.0 mg, 4.2×10^{-5} mol), $Pd(PPh_3)_4$ (12.8 mg, 1.1×10^{-5} mol), CuI (1.1 mg, 5.8×10^{-6} mol) and dry THF (5.0 mL) were added to a 100-mL round-bottom flask. Ar was bubbled into the reaction mixture for 5 min before piperidine (0.20 mL) was added. The reaction mixture was stirred at 45 °C for 24 h under Ar. After the solvent was evaporated, the residue was chromatographed on silica gel with 8:1 hexanes: THF as the eluent. Yield 22.0 mg (33% based on 41.0 mg of (5,15-diethynyl-10,20-bis[2′,6′-bis(3″,3″-dimethyl-1″-butyloxy) phenyl]porphinato)zinc(II)). ^{1}H NMR (300 MHz; $CDCl_3$): δ, ppm 9.94 (d, 4H, J = 4.6 Hz, β-H), 8.86 (d, 4H, J = 4.6 Hz, β-H), 8.07 (d, 2H, J = 8.2 Hz, Ph-H), 7.70 (t, 2H, J = 8.4 Hz, Ph-H), 7.00 (d, 4H, J = 8.5 Hz, Ph-H), 6.59 (d, 2H, J = 8.3 Hz, Ph-H), 3.91 (t, 8H, J = 7.2 Hz, –O–CH_2–C), 3.86 (t, 8H, J = 8.3 Hz, –N–CH_2–C), 1.79 (m, 8H, –N–C–CH_2–C), 1.1–1.5 (m, 24H, –CH_2–), 0.94 (t, 8H, J = 7.0 Hz, O–C–CH_2–), 0.88 (t, 12H, J = 7.2 Hz, –CH_3), 0.26 (s, 36H, –C–CH_3). MS (MALDI-TOF): m/z 1607.08 (calcd. for $[M]^+$ 1606.838).

4-Bromo-7-(4′-*n*-dodecyloxyphenylethynyl) benzo[c][1,2,5]thiadiazole. 4-*n*-Dodecyloxyethynylbenzene [99] (0.620 g, 2.16×10^{-3} mol), 4,7-dibromobenzo[c][1,2,5]thiadiazole (1.91 g, 6.50×10^{-3} mol), $Pd(PPh_3)_2Cl_2$ (0.162 g, 2.31×10^{-4} mol), CuI (21 mg, 1.1×10^{-4} mol), and dry toluene (10 mL) were added to a 100-mL round-bottom flask. Ar was bubbled into the reaction mixture for 5 min before triethylamine (10 mL) was added. The reaction mixture was stirred at 45 °C for 3 h under Ar. After the solvent was evaporated, the reaction mixture was chromatographed on silica gel with 2:1 hexanes:CH_2Cl_2. Yield 0.496 g (46% based on 0.620 g of 4-*n*-dodecyloxyethynylbenzene). ^{1}H NMR (300 MHz; $CDCl_3$): δ, ppm 7.83 (d, 1H, J = 7.6 Hz, Ph-H), 7.63 (d, 1H, J = 7.6 Hz, Ph-H), 7.59 (d, 2H, J = 8.9 Hz, Ph-H), 6.91 (d, 2H, J = 8.9 Hz, Ph-H), 3.99 (t, 2H, J = 6.6 Hz, –OCH_2–), 1.80 (quint, 2H, –OC–CH_2–), 1.45 (m, 2H,

–CH_2–), 1.2–1.4 (m, 16H, –CH_2–), 0.88 (t, 3H, J = 6.7 Hz, –CH_3). MS (CI): m/z 498.133 (calcd. for $[M]^+$ 498.134).

(5,15-Bis([7′-(4″-*n*-dodecyloxyphenylethynyl) benzo[c][1′,2′,5′]thiadiazol-4′-yl]ethynyl)-10,20-bis[2′,6′-bis(3″,3″-dimethyl-1″-butyloxy)phenyl] porphinato)zinc(II) (6). 4-Bromo-7-(4′-*n*-dodecyloxyphenylethynyl)benzo[c][1,2,5]thiadiazole (40.9 mg, 8.19×10^{-5} mol), (5,15-diethynyl-10,20-bis[2′,6′-bis-(3″,3″-dimethyl-1″-butyloxy)phenyl]porphinato)zinc(II) (35.7 mg, 3.66×10^{-5} mol), $Pd(PPh_3)_4$ (10.1 mg, 8.7×10^{-6} mol), CuI (1.3 mg, 6.8×10^{-6} mol), and dry THF (6.0 mL) were added to a 100-mL round-bottom flask. Ar was bubbled into the reaction mixture for 10 min before piperidine (0.50 mL) was added. The reaction mixture was stirred at 44 °C for 17.5 h under Ar. After cooling, the solvent was evaporated. The residue was chromatographed on silica gel with 5:1 hexanes:THF as the eluent. The product was further purified by size exclusion column chromatography (BioRad Bio-Beads SX-1 packed in THF, gravity flow). Yield 45.5 mg (69% based on 35.7 mg of 5,15-diethynyl-10,20-bis[2′,6′-bis(3″,3″-dimethyl-1″-butyloxy)phenyl]porphinato) zinc(II)). ^{1}H NMR (300 MHz; 1 drop pyridine-d_5 in $CDCl_3$): δ, ppm 9.90 (d, 4H, J = 4.6 Hz, β-H), 8.86 (d, 4H, J = 4.6 Hz, β-H), 8.15 (d, 2H, J = 7.4 Hz, Ph-H), 7.92 (d, 2H, J = 7.4 Hz, Ph-H), 7.72 (t, 2H, J = 8.4 Hz, Ph-H), 7.65 (d, 4H, J = 8.8 Hz, Ph-H), 7.03 (d, 4H, J = 8.5 Hz, Ph-H), 6.94 (d, 4H, J = 8.9 Hz, Ph-H), 4.01 (t, 4H, J = 6.6 Hz, –O–CH_2–C), 3.93 (t, 8H, J = 7.5 Hz, –O–CH_2–C), 1.82 (quint, 4H, J = 6.8 Hz, –O–CH_2–C), 1.48 (m, 4H, –CH_2–), 1.15–1.40 (m, 32H, –CH_2–), 0.89 (t, 6H, J = 6.7 Hz, –CH_3), 0.83 (t, 8H, J = 7.5 Hz, –OC–CH_2–), 0.37 (s, 36H, –C–CH_3). MS (MALDI-TOF): m/z 1809.0 (calcd. for $[M]^+$ 1808.869).

4-*n*-Dodecyloxyphenyl-4′,4′,5′,5′-tetramethyl-1′,3′,2′-dioxaborolane. 4-*n*-Dodecyloxyiodobenzene [99] (1.00 g, 2.58×10^{-3} mol), dichloro[1,1′-bis(diphenylphosphino)ferrocene]palladium(II)·dichloromethane adduct (0.106 g, 1.30×10^{-4} mol) were added to 1,2-dichloroethane (5.0 mL) and Et_3N (1.0 mL, 7.2×10^{-3} mol). 4,4,5,5-Tetramethyl-1,3,2-dioxaborolane (0.56 mL, 3.9×10^{-3} mol) was added, and the reaction mixture was stirred at 75 °C for 1.5 h under Ar. After cooling, the solvent was evaporated. The residue was chromatographed on silica gel with 2:1 hexanes:$CHCl_3$ as the eluent. Yield 0.674 g (67% based on 1.00 g of 4-*n*-dodecyloxyiodobenzene). ^{1}H NMR (250 MHz; $CDCl_3$): δ, ppm 7.73 (d, 2H, J = 8.7 Hz, Ph-H), 6.88 (d, 2H, J = 8.7 Hz, Ph-H), 3.97 (t, 2H, J = 6.6 Hz, –OCH_2–), 1.78 (quint, 2H, J = 6.6 Hz, –OC–CH_2–), 1.45 (m, 2H, –CH_2–), 1.33 (s, 12H, –CH_3), 1.26 (m, 16H, –CH_2–), 0.88 (t, 3H, J = 6.5 Hz, –CH_3). MS (CI): m/z 388.317 (calcd. for $[M]^+$ 388.315).

4-Bromo-7-(4′-*n*-dodecyloxyphenyl)benzo[c][1,2,5] thiadiazole. 4-*n*-Dodecyloxyphenyl-4′,4′,5′,5′-tetramethyl-1′,3′,2′-dioxaborolane (0.313 g, 8.06×10^{-4} mol), 4,7-dibromobenzo[c][1,2,5]thiadiazole (0.474 g, 1.61×10^{-3} mol), $Pd(PPh_3)_4$ (97 mg, 8.4×10^{-5} mol), K_2CO_3 (0.347 g, 2.51×10^{-3} mol), DMF (25 mL), and H_2O (3.0 mL) were added to a 100-mL round-bottom flask. Ar was bubbled into the reaction mixture for 5 min at room temperature. The reaction mixture was warmed up to 86 °C and stirred for 7.5 h under Ar. After cooling, 200 mL of dilute aq. HCl was added to the reaction mixture, and the product was extracted with $CHCl_3$ and dried over Na_2SO_4. The solvent was evaporated, and the residue was chromatographed on silica gel with 1:1 hexanes:$CHCl_3$. The product was further purified by size exclusion column chromatography (BioRad Bio-Beads SX-1 packed in THF, gravity flow). Yield 0.295 g (77% based on 0.313 g of 4-*n*-dodecyloxyphenyl-4′,4′,5′,5′-tetramethyl-1′,3′,2′-dioxaborolane). ^{1}H NMR (300 MHz; $CDCl_3$): δ, ppm 7.90 (d, 1H, J = 7.6 Hz, –CH_2–), 7.85 (d, 2H, J = 8.8 Hz, Ph-H), 7.53 (d, 1H, J = 7.6 Hz, Ph-H), 7.05 (d, 2H, J = 8.8 Hz, Ph-H), 4.04 (t, 2H, J = 6.5 Hz, –OCH_2–), 1.83 (quint, 2H, J = 6.5 Hz, –OC–CH_2–), 1.49 (m, 2H, –CH_2–), 1.2–1.4 (m, 16H, –CH_2–), 0.88 (t, 3H, J = 6.6 Hz, –CH_3). MS (CI): m/z 474.133 (calcd. for $[M]^+$ 474.134).

4-(4′-*n*-Dodecyloxyphenyl)-7-(trimethylsilylethynyl)benzo[c][1,2,5]thiadiazole. 4-Bromo-7-(4′-*n*-dodecyloxyphenyl)benzo[c][1,2,5]thiadiazole (0.2364 g, 4.97×10^{-4} mol), $Pd(PPh_3)_4$ (55.4 mg, 4.79×10^{-5} mol), CuI (3.4 mg, 1.8×10^{-5} mol), and dry THF (10 mL) were added to a 100-mL round-bottom flask. Ar was bubbled into the reaction mixture for 5 min before (trimethylsilyl)acetylene (0.25 mL, 1.8×10^{-3} mol) and diisopropylamine (1.0 mL) were added. The reaction mixture was stirred at 50 °C for 17.5 h under Ar. After cooling, the solvent was evaporated. The residue was chromatographed on silica gel with 8:1 hexanes:THF. Yield 0.240 g (98% based on 0.2364 g of 4-bromo-7-(4′-*n*-dodecyloxyphenyl)benzo[c][1,2,5]thiadiazole). ^{1}H NMR (300 MHz; $CDCl_3$): δ, ppm 7.90 (d, 2H, J = 8.9 Hz, Ph-H), 7.82 (d, 1H, J = 7.4 Hz, Ph-H), 7.61 (d, 1H, J = 7.4 Hz, Ph-H), 7.05 (d, 2H, J = 8.9 Hz, Ph-H), 4.04 (t, 2H, J = 6.5 Hz, –OCH_2–), 1.82 (quint, 2H, J = 6.9 Hz, –OC–CH_2–), 1.49 (m, 2H, –CH_2–), 1.2–1.4 (m, 16H, –CH_2–), 0.88 (t, 3H, J = 6.7 Hz, –CH_3), 0.34 (s, 9H, –Si–CH_3). MS (CI): m/z 493.272 (calcd. for $[M + H]^+$ 493.271).

4-(4′-*n*-Dodecyloxyphenyl)-7-ethynylbenzo[c][1,2,5] thiadiazole. 4-(4′-*n*-Dodecyloxyphenyl)-7-(trimethylsilylethynyl)benzo[c][1,2,5]thiadiazole (0.223 g, 4.53×10^{-4} mol) was dissolved in a mixture of THF (7.0 mL) and MeOH (3.0 mL). K_2CO_3 (85 mg, 6.2×10^{-4} mol) was added, and the reaction mixture was stirred for 2 h under Ar. The reaction mixture was filtered and the filtrate evaporated. Yield 0.190 g (99.7% based on 0.223 g of 4-(4′-*n*-dodecyloxyphenyl)-7-(trimethylsilylethynyl) benzo[c][1,2,5]thiadiazole). ^{1}H NMR (300 MHz; $CDCl_3$): δ, ppm 7.90 (d, 2H, J = 8.9 Hz, Ph-H), 7.86 (d, 1H, J = 7.3 Hz, Ph-H), 7.63 (d, 1H, J = 7.4 Hz, Ph-H), 7.06 (d, 2H, J = 8.9 Hz, Ph-H), 4.04 (t, 2H, J = 6.5 Hz, –OCH_2–), 3.60 (s, 1H, ethynyl-H), 1.83 (quint, 2H,

J = 6.9 Hz, –OC–CH_2–), 1.49 (m, 2H, –CH_2–), 1.2–1.4 (m, 16H, –CH_2–), 0.88 (t, 3H, J = 6.7 Hz, –CH_3). MS (ESI): m/z 421.233 (calcd. for $[M + H]^+$ 421.231).

4-([4′-(4″-*n*-Dodecyloxyphenyl)benzo[c][1′,2′,5′]thiadiazol-7′-yl]ethynyl)-7-iodobenzo[c][1,2,5]thiadiazole. 4-(4′-*n*-Dodecyloxyphenyl)-7-ethynylbenzo[c][1,2,5]thiadiazole (0.120 g, 2.85×10^{-4} mol), 4,7-diiodobenzo[c][1,2,5]thiadiazole [99] (0.232 g, 5.98×10^{-4} mol), Pd_2dba_3 (32.8 mg, 3.6×10^{-5} mol), $AsPh_3$ (92.4 mg, 3.0×10^{-4} mol), and dry THF (15 mL) were added to a 100-mL round-bottom flask. Ar was bubbled into the reaction mixture for 5 min before diisopropylethylamine (1.0 mL) was added. The reaction mixture was stirred at 48 °C for 12.5 h under Ar. After cooling, the solvent was evaporated. The residue was chromatographed on silica gel with 8:1 hexanes:THF. The product was further purified by size exclusion column chromatography (BioRad Bio-Beads SX-1 packed in THF, gravity flow). Yield 69.8 mg (36% based on 0.120 g of 4-(4′-*n*-dodecyloxyphenyl)-7-ethynylbenzo[c][1,2,5]thiadiazole). ^{1}H NMR (300 MHz; $CDCl_3$): δ, ppm 8.16 (d, 1H, J = 7.5 Hz, Ph-H), 8.03 (d, 1H, J = 7.4 Hz, Ph-H), 7.96 (d, 2H, J = 8.9 Hz, Ph-H), 7.71 (d, 1H, J = 7.4 Hz, Ph-H), 7.70 (d, 1H, J = 7.5 Hz, Ph-H), 7.08 (d, 2H, J = 8.9 Hz, Ph-H), 4.05 (t, 2H, J = 6.5 Hz, –OCH_2–), 1.84 (quint, 2H, J = 7.0 Hz, –OC–CH_2–), 1.49 (m, 2H, –CH_2–), 1.2–1.4 (m, 16H, –CH_2–), 0.88 (t, 3H, J = 6.6 Hz, –CH_3). MS (MALDI-TOF): m/z 680.09 (calcd. for $[M]^+$ 680.110).

(5,15-Bis([7′-([7″-(4‴-*n*-dodecyloxyphenyl)benzo[c][1″,2″,5″]thiadiazol-4″-yl]ethynyl)benzo[c][1′,2′,5′]thiadiazol-4′-yl]ethynyl)-10,20-bis[2′,6′-bis(3″,3″-dimethyl-1″-butyloxy)phenyl]porphinato)zinc(II) (7). 4-([4′-(4″-*n*-Dodecyloxyphenyl)benzo[c][1′,2′,5′]thiadiazol-7′-yl]ethynyl)-7-iodobenzo[c][1,2,5]thiadiazole (31.0 mg, 4.55×10^{-5} mol), 5,15-diethynyl-10,20-bis[2′,6′-bis(3″,3″-dimethyl-1″-butyloxy)phenyl]porphinato)zinc(II) (22.2 mg, 2.28×10^{-5} mol), $Pd(PPh_3)_4$ (9.1 mg, 7.9×10^{-6} mol), CuI (1.7 mg, 8.9×10^{-6} mol), and dry THF (8.0 mL) were added to a 100-mL round-bottom flask. Ar was bubbled into the reaction mixture for 5 min before piperidine (0.50 mL) was added. The reaction mixture was stirred at 50 °C for 3.5 h under Ar. After cooling, the solvent was evaporated. The residue was chromatographed on silica gel with 3:1 hexanes:THF as the eluent. The product was further purified by size exclusion column chromatography (BioRad Bio-Beads SX-1 packed in THF, gravity flow). Yield 30.2 mg (64% based on 31.0 mg of 4-([4′-(4″-*n*-dodecyloxyphenyl)benzo[c][1′,2′,5′]thiadiazol-7′-yl]ethynyl)-7-iodobenzo[c][1,2,5]thiadiazole). ^{1}H NMR (300 MHz; 1 drop pyridine-d_5 in $CDCl_3$): δ, ppm 9.92 (d, 4H, J = 4.6 Hz, β-H), 8.89 (d, 4H, J = 4.5 Hz, β-H), 8.21 (d, 2H, J = 7.4 Hz, Ph-H), 8.13 (d, 2H, J = 7.4 Hz, Ph-H), 8.09 (d, 2H, J = 7.4 Hz, Ph-H), 7.98 (d, 4H, J = 8.7 Hz, Ph-H), 7.75 (d, 2H, J = 7.3 Hz, Ph-H), 7.73 (t, 2H, J = 8.3 Hz, Ph-H), 7.09 (d, 4H, J = 8.8 Hz, Ph-H), 7.04 (d, 4H, J = 8.5 Hz, Ph-H), 4.06 (t, 4H, J = 6.4 Hz, –O–CH_2–C), 3.94 (t, 8H, J = 7.5 Hz, –O–CH_2–C), 1.85 (quint, 4H, J = 7.0 Hz, –O–CH_2–C), 1.50 (m, 4H, –CH_2–), 1.15–1.40 (m, 32H, –CH_2–), 0.89 (t, 6H, –CH_3), 0.85 (t, 8H, J = 7.5 Hz, –OC–CH_2–), 0.39 (s, 36H, –C–CH_3). MS (MALDI-TOF): m/z 2076.99 (calcd. for $[M]^+$ 2076.857).

5,15-Bis([7′-(4″-*N*,*N*-dihexylaminophenylethynyl)benzo[c][1′,2′,5′]thiadiazol-4′-yl]ethynyl)-10,20-bis[2′,6′-bis(3″,3″-dimethyl-1″-butyloxy)phenyl]porphinato)zinc(II) (8). 4-(4′-*N*,*N*-Dihexylaminophenylethynyl)-7-iodobenzo[c][1,2,5]thiadiazole [99] (73.6 mg, 1.35×10^{-4} mol), 5,15-diethynyl-10,20-bis[2′,6′-bis(3″,3″-dimethyl-1″-butyloxy)phenyl]porphinato)zinc(II) (59.0 mg, 6.05×10^{-5} mol), $Pd(PPh_3)_4$ (15.6 mg, 1.35×10^{-5} mol), CuI (1.0 mg, 5.3×10^{-6} mol), and dry THF (6.0 mL) were added to a 100-mL round-bottom flask. Ar was bubbled into the reaction mixture for 5 min before piperidine (0.50 mL) was added. The reaction mixture was stirred at 49 °C for 20 h under Ar. After cooling, the solvent was evaporated. The residue was chromatographed on silica gel with 5:1 hexanes:THF as the eluent. The product was further purified by size exclusion column chromatography (BioRad Bio-Beads SX-1 packed in THF, gravity flow). Yield 0.107 g (98% based on 59.0 mg of 5,15-diethynyl-10,20-bis[2′,6′-bis(3″,3″-dimethyl-1″-butyloxy)phenyl]porphinato)zinc(II)). ^{1}H NMR (300 MHz; $CDCl_3$): δ, ppm 9.99 (d, 4H, J = 4.6 Hz, β-H), 8.94 (d, 4H, J = 4.6 Hz, β-H), 8.17 (d, 2H, J = 7.4 Hz, Ph-H), 7.89 (d, 2H, J = 7.4 Hz, Ph-H), 7.73 (t, 2H, J = 8.4 Hz, Ph-H), 7.56 (d, 4H, J = 7.7 Hz, Ph-H), 7.03 (d, 4H, J = 8.5 Hz, Ph-H), 6.64 (d, 4H, J = 9.0 Hz, Ph-H), 3.94 (t, 8H, J = 7.3 Hz, –O–CH_2–C), 3.32 (t, 8H, J = 7.6 Hz, –N–CH_2–C), 1.5–1.7 (m, 4H, –CH_2–), 1.25–1.45 (m, 24H, –CH_2–), 0.8–1.0 (m, 20H, –O–C–CH_2– and –CH_3), 0.26 (s, 36H, –C–CH_3). MS (MALDI-TOF): m/z 1807.1 (calcd. for $[M]^+$ 1806.901).

4-(4′-(*N*,*N*-Dihexylamino)phenylethenyl)-7-iodobenzo[c][1,2,5]thiadiazole. *N*,*N*-Dihexylamino-4-vinylbenzene [99] (0.154 g, 5.36×10^{-4} mol), 4,7-diiodobenzo[c][1,2,5]thiadiazole [99] (0.309 g, 7.96×10^{-4} mol), Pd_2dba_3 (50.4 mg, 5.5×10^{-5} mol), and dry 1,4-dioxane (7.0 mL) were added to a 100-mL round-bottom flask. Ar was bubbled into the reaction mixture for 5 min before dicyclohexylmethylamine (0.50 mL) and $P(t\text{-}Bu)_3$ (10 wt% in hexanes, 1.00 mL, 3.3×10^{-4} mol) were added. The reaction mixture was stirred at 57 °C for 48 h under Ar. After the solvent was evaporated, the reaction mixture was chromatographed on silica gel with 8:1 hexanes:THF. The product was further purified by size exclusion column chromatography (BioRad Bio-Beads SX-1 packed in THF, gravity flow). Yield 42.2 mg (14% based on 0.154 g of *N*,*N*-dihexylamino-4-vinylbenzene). ^{1}H NMR (300 MHz; $CDCl_3$): δ, ppm 8.04 (d, 1H, J = 7.6 Hz, Ph-H), 7.84 (d, 1H, J = 16.4 Hz, vinyl-H), 7.50 (d, 2H, J = 8.8 Hz, Ph-H), 7.38 (d, 1H, J = 16.2 Hz, vinyl-H), 7.37 (d, 1H, J = 7.8 Hz, Ph-H), 6.64 (d, 2H, J = 8.9 Hz, Ph-H), 3.30 (t, 4H, J = 7.6 Hz, –NCH_2–), 1.61 (m, 4H,

–NC–CH_2–), 1.15–1.45 (m, 12H, –CH_2–), 0.91 (t, 6H, J = 6.7 Hz, –CH_3). MS (CI): m/z 547.1481 (calcd. for $[M]^+$ 547.148).

(5,15-Bis([7′-(4″-*N*,*N*-dihexylaminophenylethenyl) benzo[c][1′,2′,5′]thiadiazol-4′-yl]ethynyl)-10,20-bis[2′,6′-bis(3″,3″-dimethyl-1″-butyloxy)phenyl] porphinato)zinc(II) (9). 4-(4′-*N*,*N*-Dihexylamino-phenylethenyl)-7-iodobenzo[c][1,2,5]thiadiazole (42.2 mg, 7.71×10^{-5} mol), 5,15-diethynyl-10,20-bis[2′,-6′-bis(3″,3″-dimethyl-1″-butyloxy)phenyl]porphinato) zinc(II) (38.0 mg, 3.90×10^{-5} mol), $Pd(PPh_3)_4$ (10.5 mg, 9.1×10^{-6} mol), CuI (1.0 mg, 5.3×10^{-6} mol), and dry THF (5.0 mL) were added to a 100-mL round-bottom flask. Ar was bubbled into the reaction mixture for 5 min before piperidine (0.50 mL) was added. The reaction mixture was stirred at 47 °C for 43 h under Ar. After cooling, the solvent was evaporated. The residue was chromatographed on silica gel with 5:1 hexanes:THF as the eluent. The product was further purified by size exclusion column chromatography (BioRad Bio-Beads SX-1 packed in THF, gravity flow). Yield 30.4 mg (43% based on 42.2 mg of 4-(4′-*N*,*N*-dihexylaminophenylethenyl)-7-iodobenzo[c][1,2,5]thiadiazole). ^{1}H NMR (500 MHz; 1 drop pyridine-d_5 in $CDCl_3$): δ, ppm 9.90 (d, 4H, J = 4.5 Hz, β-H), 8.84 (d, 4H, J = 4.5 Hz, β-H), 8.14 (d, 2H, J = 7.2 Hz, Ph-H), 7.99 (d, 2H, J = 16.1 Hz, vinyl-H), 7.77 (d, 2H, J = 7.4 Hz, Ph-H), 7.71 (t, 2H, J = 8.5 Hz, Ph-H), 7.57 (d, 4H, J = 8.4 Hz, Ph-H), 7.55 (d, 2H, J = 16.0 Hz, vinyl-H), 7.02 (d, 4H, J = 8.6 Hz, Ph-H), 6.68 (d, 4H, J = 8.7 Hz, Ph-H), 3.92 (t, 8H, J = 7.4 Hz, –O–CH_2–C), 3.33 (t, 8H, J = 7.6 Hz, –N–CH_2–C), 1.63 (m, 8H, –CH_2–), 1.3–1.4 (m, 24H, –CH_2–), 0.93 (t, 12H, J = 6.7 Hz, –CH_3), 0.84 (t, 8H, J = 7.5 Hz, –O–C–CH_2–), 0.39 (s, 36H, –C–CH_3). MS (MALDI-TOF): m/z 1811.0 (calcd. for $[M]^+$ 1810.932).

RESULTS AND DISCUSSION

Synthesis

Chromophores **2–9** are based on a (5,15-diethynylporphinato)zinc(II) framework and feature symmetric donor or acceptor units appended at the *meso*-ethynyl positions that derive from phenylene and benzo[c][1,2,5]thiadiazole building blocks; these structures, along with the TMS-protected (5,15-diethynyl-10,20-bis[3′,5′-bis(9″-methoxy-1″,4″,7″-trioxanonyl)phenyl] porphinato)zinc(II) reference monomer (**1**), are shown in Fig. 1. Scheme 1 details the syntheses of fluorophores **3–9**. The proquinoidal spacer unit, benzo[c][1,2,5]thiadiazole, which extends π-conjugation from the porphyrin core for **4–9**, has been used not only as a common building block to enhance electronic delocalization within π-conjugated oligomers and polymers, but also as an electron accepting moiety [55, 99, 101, 102]. Incorporation of benzo[c][1,2,5] thiadiazole into conjugated organic networks is made facile through the agency of palladium-catalyzed cross-coupling reactions. In **2–9**, each aromatic unit is linked by either ethyne or ethene units through Sonogashira or Heck coupling reactions. The 10- and 20-*meso*-positions of the (porphinato)zinc cores of **1–9** feature either 3,5-bis(9′-methoxy-1′,4′,7′-trioxanonyl)phenyl (**1**) or 2,6-bis(3′,3′-dimethyl-1′-butyloxy)phenyl substituents (**2–9**) to ensure high solubility. Fluorophores **2–9** were synthesized by Pd-mediated cross-coupling reactions involving appropriately modified terminal substituents and 5,15-dibromo- or 5,15-diethynyl(porphinato)zinc(II) synthons (Experimental Section).

Steady-state electronic absorption spectra

Electronic absorption spectra of NIR fluorophores **2–9** recorded in THF solvent are displayed in Fig. 2. These chromophores feature lowest energy Q absorption bands that are significantly red-shifted (1985–3070 cm^{-1}) and intensified (~20 to 50-fold enhanced in oscillator strength) relative to the analogous transition manifold of [5,10,15,20-tetraphenyl(porphinato)]zinc(II) (**TPPZn**) [100]. While chromophores **2** and **3** manifest spectral signatures akin to other closely related, [5,15-bis[(aryl) ethynyl]-10,20-diphenylporphinato]zinc(II) complexes [42], note that structures **4–9**, which incorporate benzo[c] [1,2,5]thiadiazole units, manifest spectra that bear distinct similarities to chlorophylls and structurally related molecules [103]. The extinction coefficients of the x-polarized Q-band [Q_x(0,0)] transitions for **4–9** are significantly enhanced relative to **2** and **3**, which bear 5,15-bis(arylethynyl) macrocycle substituents (Fig. 2, Table 1). As conjugation is expanded at the porphyrin (5,15-bis(benzo[c][1′,2′,5′]thiadiazol-4′-ylethynyl) moieties [**4**→**5**→(**6**, **7**, **8**, **9**)] (Fig. 2, Table 1), increasingly pronounced B-state (Soret) transition manifold splitting is evident; note that the Q_x(0,0) transition extinction coefficients for fluorophores **6–9** surpass those of their most intense respective B-band absorption, and exceed 10^5 $M^{-1}.cm^{-1}$, a value comparable to Q-state absorptions characteristic of chlorophylls and phthalocyanines [30, 37]. In contrast to the full widths at half maximum (FWHM) values for the B-band manifolds of **6–9**, which span 4430–6480 cm^{-1} and greatly exceed that of the **TPPZn** benchmark (660 cm^{-1}), the FWHMs of their respective Q_x(0,0) transitions range from 812 to 940 cm^{-1}. Compounds **3** and **8** highlight the qualitative impact of 5,15-bis(benzo[c][1′,2′,5′]thiadiazol-4′-ylethynyl) substituents relative to corresponding 5,15-bis[(aryl)ethynyl] groups upon the (porphinato)zinc chromophore long-wavelength absorption maximum: note the x-polarized Q-state absorption maximum for **8** is 928 cm^{-1} red-shifted relative to that for **3**. The enhanced π–conjugation afforded by the benzo[c][1,2,5] thiadiazolyl group is consistent with its proquinoidal character [104], and earlier work which establishes that *meso* (benzo[c][1,2,5]thiadiazol-4-ylethynyl) substituents

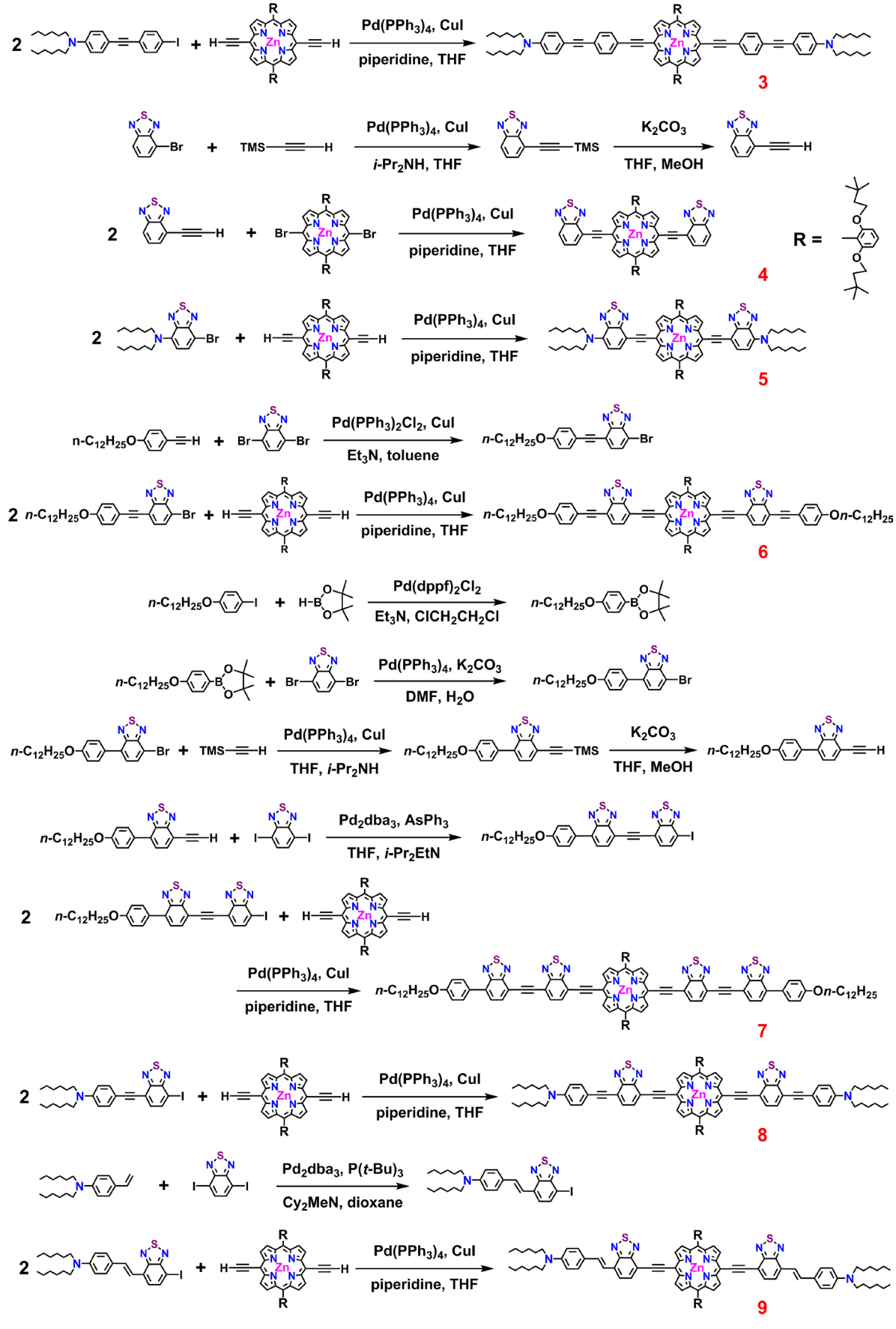

Scheme 1. Synthetic routes to 5,15-diethynyl-(porphinato)zinc(II)-based fluorophores **3**–**9** and to key precursor compounds

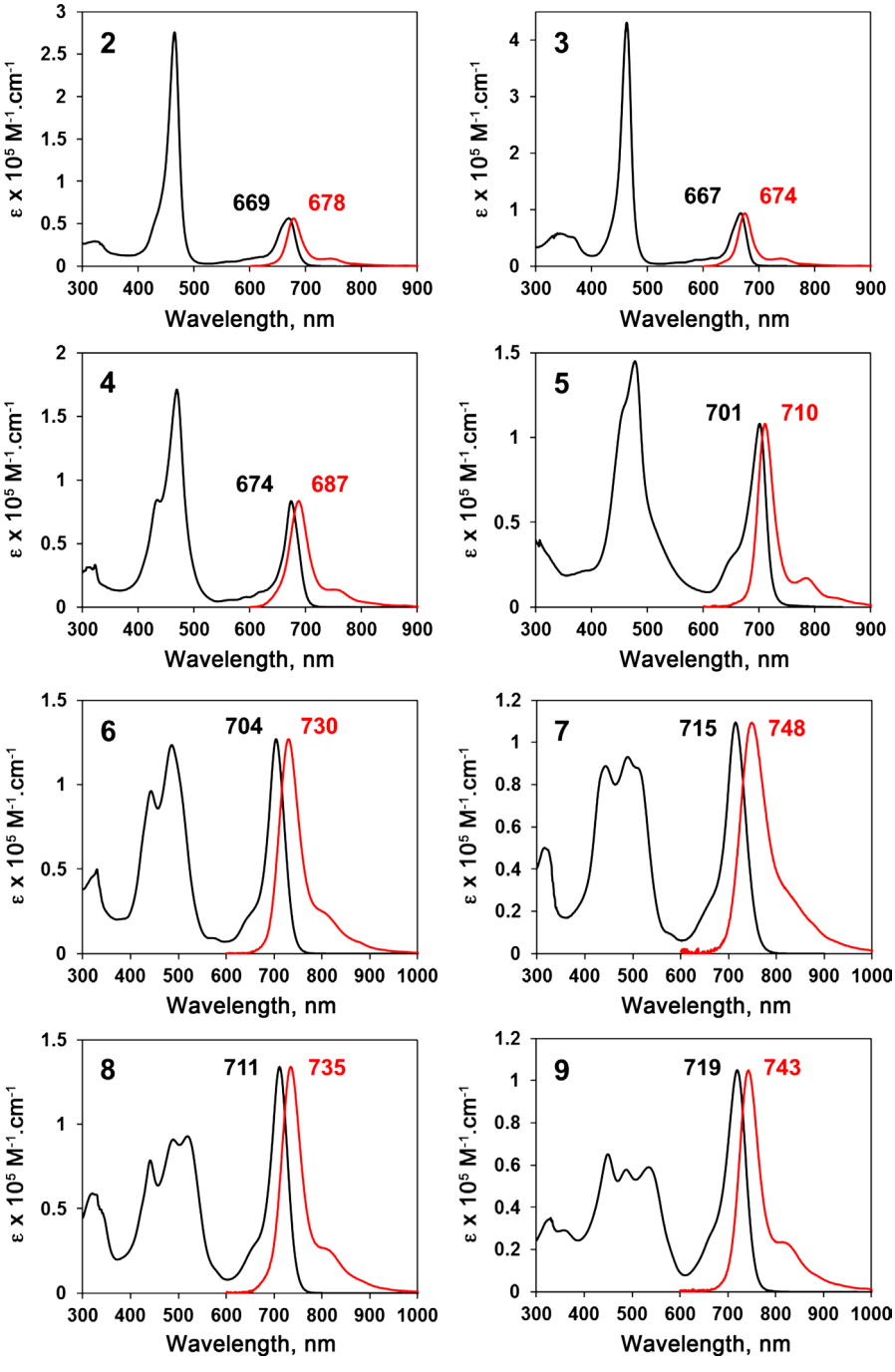

Fig. 2. Absorption (black line) and fluorescence (red line) spectra of 5,15-diethynyl-(porphinato)zinc(II)-based fluorophores **2–9** recorded in THF solvent

drive pronounced S_1 state cumulenic character for (porphinato)zinc-based chromophores [55].

Fluorescence spectra

Figure 2 also highlights the fluorescence spectra recorded for chromophores **2–9** in THF solvent; these spectra mirror the respective lowest energy Q-state absorption manifolds for these chromophores. The fluorescence energy maxima red-shift with increasing degrees of conjugation [**4**→**5**→(**6**, **7**, **8**, **9**)] (Fig. 2, Table 1); note in this regard that fluorophore **7** features an emission band maximum centered at 748 nm, and that structures **2–9** feature narrow fluorescence bands ($620\ cm^{-1} < FWHM(S_1 \rightarrow S_0) < 1130\ cm^{-1}$) that are significantly reduced with respect to the $S_1 \rightarrow S_0$ FWHM value determined for **TPPZn** ($1924\ cm^{-1}$). Note also that the narrow fluorescence bands of **2–9** resemble the spectral breadths of their respective lowest energy Q-state absorption manifolds (Table 1) and feature low-magnitude

Table 1. Comparative electronic absorption and steady-state fluorescence spectral data determined for chromophores **1–9** in THF solvent relative to the **TPPZn** benchmark

	λ_{max} ($S_0 \rightarrow S_1$), nm[a]	ε_{max} ($S_0 \rightarrow S_1$), $M^{-1}.cm^{-1}$[a]	FWHM ($S_0 \rightarrow S_1$), cm^{-1}[a]	λ_{max} ($S_1 \rightarrow S_0$), nm	FWHM ($S_1 \rightarrow S_0$), cm^{-1}	Stokes shift, cm^{-1}[c]
TPPZn (in benzene)	589	3680	577	605	1924[b]	449
1	632	33,200	438	638	626	149
2	669	57,000	824	678	656	198
3	667	94,000	704	674	618	156
4	674	84,000	654	687	809	281
5	701	108,000	737	710	649	181
6	704	127,000	812	730	922	506
7	715	109,400	939	748	1131	617
8	711	134,000	818	735	890	459
9	719	105,000	940	743	870	449

[a]For **1–9**, the value reported corresponds to that for the x-polarized ($S_0 \rightarrow S_1$) absorption. Note that for the **TPPZn** chromophore, the value reported corresponds to that for the Q(0,0) transition. [b]The value reported corresponds to that for the Q-state manifold. [c]The difference in energy between the absorption ($S_0 \rightarrow S_1$) and fluorescence ($S_1 \rightarrow S_0$) band maxima.

Table 2. Comparative x-polarized [$S_0 \rightarrow S_1$; $Q_x(0,0)$] integrated absorptive oscillator strengths, fluorescence quantum yields, fluorescence lifetimes, experimental and calculated radiative rate constants, and experimental non-radiative rate constants determined for chromophores **1–9** in THF solvent relative to the **TPPZn** benchmark

	Oscillator strength[a]	Φ_f[b]	τ_f, ns	k_r ($\times 10^7$ s^{-1})	k_{nr} ($\times 10^7$ s^{-1})	k_r(calc)[d] ($\times 10^7$ s^{-1})
TPPZn (in benzene)	0.00977	0.033[c]	2.09	1.58	46.27	1.78
1	0.0669	0.058 (0.021)	1.99	2.91	47.34	4.30
2	0.216	0.22 (0.044)	2.04	10.78	38.24	7.72
3	0.304	0.25 (0.043)	1.63	15.34	46.01	11.1
4	0.253	0.15 (0.013)	1.42	10.56	59.86	9.23
5	0.366	0.19 (0.012)	1.20	15.83	67.50	11.3
6	0.474	0.32 (0.020)	1.97	16.24	34.52	13.0
7	0.473	0.35 (0.035)	1.87	18.72	34.76	11.8
8	0.504	0.36 (0.032)	1.71	21.05	37.43	13.8
9	0.454	0.26 (0.029)	1.37	18.98	54.01	11.5

[a]$f = 4.6 \times 10^{-9} \cdot \varepsilon_{max} \cdot \Delta\nu_{1/2}$; the oscillator strengths were calculated for the x-polarized ($S_0 \rightarrow S_1$) absorption. Note that for the **TPPZn** chromophore, the reported integrated oscillator strength corresponds to that for the Q-state transition manifold. [b]Fluorescence quantum yields determined relative to free base TPP in benzene ($\Phi_f = 0.13$); parenthetical values represent standard deviations from the mean. [c]From Ref. 100. [d]Calculated using Equation 2.

Stokes shifts (155–620 cm^{-1}), congruent with a minimal degree of excited-state structural relaxation relative the ground-state conformation for these chromophores.

Strickler–Berg analysis of the S_1-state photophysics of fluorophores 2–9

Relative to the (porphinato)zinc chromophore **TPPZn** (Φ_f = 0.033), the fluorescence quantum yields of fluorophores **2–9** are particularly dramatic (0.15 < Φ_f < 0.36; Table 2). Further, given the shape and intensity of the steady-state fluorescence spectra of these monomeric (porphinato)zinc chromophores that bear either 5,15-bis[(aryl)ethynyl] or 5,15-bis(benzo[c][1′,2′,5′]thiadiazol-4′-ylethynyl) substituents, coupled with the fact that the emission band maxima of these species are significantly red-shifted (1690–3160 cm^{-1}) with respect to the **TPPZn** benchmark (Table 1), suggest an analysis of the S_1 state photophysics within the context of the Strickler–Berg model, which relates increases in

the integrated oscillator strength of the lowest-energy ground-state absorption band with a corresponding augmentation of the radiative decay rate constant (k_r, Equation 2) [22].

$$k_r = 2.880\times10^{-9} n^2 \left\langle \tilde{\nu}_f^{-3} \right\rangle_{Av}^{-1} \frac{g_l}{g_u} \int \varepsilon d \ln \tilde{\nu} \qquad (2)$$

Here k_r is radiative decay rate constant, n is the refractive index of the solvent, g_l and g_u are the respective degeneracies of the ground and excited states, ε is the molar extinction coefficient, ν is the frequency of the transition in cm^{-1}. The term $\langle \tilde{\nu}_f^{-3} \rangle_{Av}^{-1}$ is expressed as;

$$\left\langle \tilde{\nu}_f^{-3} \right\rangle_{Av}^{-1} = \frac{\int I(\nu) d\nu}{\int \nu^{-3} I(\nu) d\nu} \qquad (3)$$

where I is the intensity of the fluorescence spectrum, measured in terms of relative numbers of quanta at each frequency. The fluorescence quantum yield (Φ_f) is simply described by Equation 4;

$$\Phi_f = \frac{k_r}{k_r + k_{nr}} \qquad (4)$$

where k_{nr} describes the magnitude of the non-radiative decay rate constant, which corresponds to the sum of the internal conversion (k_{ic}) and intersystem crossing (k_{isc}) rate constants. Provided that the magnitudes of the non-radiative rate remain approximately constant within a family of closely related chromophores, an increase in the integrated oscillator strength results in a corresponding increase in the fluorescence quantum yield.

Figure 3 highlights the x-polarized Q-state oscillator strength dependent fluorescence quantum yields, radiative rate constants, and non-radiative rate constants of fluorophores **1–9** relative to the **TPPZn** benchmark. Note the distinct increase in the magnitude of the radiative rate constant with increasing x-polarized Q-state oscillator strength (Fig. 3B), and that the measured k_r values for fluorophores **5–9** exceed that of the **TPPZn** by more than an order of magnitude. This apparent Stricker–Berg dependence of the radiative rate constant upon the integrated lowest energy $S_0 \rightarrow S_1$ oscillator strength gives rise to a family of porphyrin-based NIR fluorophores in which the longest wavelength emitter (**7**, 748 nm) features a fluorescence quantum yield ($\Phi_f = 0.35$; Tables 1 and 2) that exceeds that of chromophores **1–6** and **9**, which emit to the blue of this wavelength.

As emission wavelengths approach the NIR spectral domain, the simple Stricker–Berg predicted dependence of the radiative rate constant upon the magnitude of the integrated oscillator strength is generally mitigated by expected energy gap law effects [23], where increasing magnitudes of the S_0–S_1 internal conversion rate constant (k_{ic}) track with diminishing S_0–S_1 energy gaps and thus sharply decrease Φ_f. In these chromophores, two factors conspire to enhance Φ_f as emission wavelength increases over the 650–750 nm spectral domain. The first of these derives from the fact that the proquinoidal benzo[c][1,2,5]thiadiazole unit minimizes the extent of excited-state structural relaxation relative the ground-state conformation [55] for chromophores **4–9**, reflected by the narrow fluorescence bands and modest Stokes shifts determined for these species (Fig. 2; Tables 1 and 2), and thereby reduces S_1–S_0 Franck–Condon overlap important for determining the magnitude of k_{ic}. The second factor that drives this unusual dependence of Φ_f upon emission wavelength stems from the fact that for these ethyne-elaborated (porphinato)zinc derivatives, intersystem

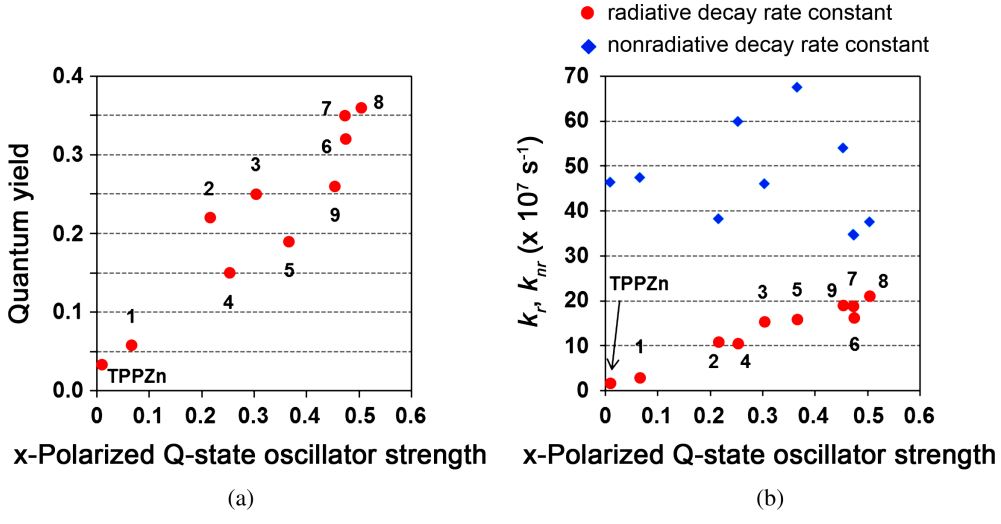

Fig. 3. x-Polarized Q-state [Q_x ($S_0 \rightarrow S_1$)] oscillator strength dependent fluorescence quantum yields, radiative rate constants (k_r), and non-radiative rate constants (k_{nr}) of diethynyl(porphinato)zinc(II) derivatives (**1–9**) relative to the [5,10,15,20-tetraphenyl-(porphinato)]zinc(II) (**TPPZn**) benchmark. (a) x-Polarized Q-state oscillator strength dependence of the fluorescence quantum yield. (b) x-Polarized Q-state oscillator strength dependence of the radiative and non-radiative decay rate constant magnitudes

crossing into the triplet manifold generates T_1 states that manifest more spatially confined excitations relative to the globally delocalized S_1 states of these chromophores [41, 45, 47, 54, 62]. This diminished overlap of S_1 and T_1 state wavefunctions mitigates S_1-T_1 intersystem crossing rate constants (k_{isc} values), and thus serves to counter-balance the effect of augmented Franck–Condon mediated internal conversion that typically accompanies S_0-S_1 energy gap reductions; this effect has been detailed previously for closely related compounds [57]. Thus, for **4–9**, extension of x-polarized conjugation of the (5,15-diethynylporphinato)zinc(II) framework *via* the benzo[c][1,2,5]thiadiazole moiety causes the magnitude of k_r to increase faster than does the magnitude of k_{nr} as emission wavelength increases, providing substantial fluorescence quantum yields that manifest a weak energy gap law [23] dependence over this spectral regime.

CONCLUSION

We describe a design strategy for (porphinato)zinc-based chromophores that possess large NIR fluorescence quantum yields. These fluorophores are based on a (5,15-diethynylporphinato)zinc(II) framework and feature symmetric donor or acceptor units appended at the *meso*-ethynyl positions *via* benzo[c][1,2,5]thiadiazole moieties. These chromophores possess red-shifted absorption and emission bands relative to **TPPZn** and (5,15-diethynyl-10,20-arylporphinato)zinc(II) benchmarks that range between 650 and 750 nm and bear distinct spectral similarities to those manifest by chlorophylls and structurally related molecules.

Interestingly, the measured radiative decay rate constants for these emitters track with the integrated oscillator strengths of their respective x-polarized Q-band absorptions, and thus define an unusual family of high quantum yield NIR fluorophores in which emission intensity is governed by a simple Strickler–Berg dependence. These photophysical properties derive from the facts that: (i) the proquinoidal benzo[c][1,2,5]thiadiazole unit minimizes the extent of excited-state structural relaxation relative the ground-state conformation [55], and (ii) *meso*-ethynyl elaborated (porphinato)zinc compounds are characterized by T_1 states that are more spatially confined than their globally delocalized S_1 states [41, 45, 47, 54, 62], which result in diminished S_1-T_1 intersystem crossing rate constants relative to conventional (porphinato)zinc chromophores. For these NIR fluorophores, these effects cause the magnitude of k_r to increase faster than does the magnitude of k_{nr} as emission wavelength increases, providing substantial fluorescence quantum yields that manifest a weak energy gap law [23] dependence over the spectral regime (685–750 nm) spanned by these emitters. These designs that take advantage of these photophysical properties make possible broadly absorptive and strongly emissive NIR fluorophores that derive from a monomeric (5,15-diethynyl-porphinato)zinc framework.

Acknowledgements

This work was supported through the Department of Defense (W81XWH-13-1-0086). The authors thank Professor Felix N. Castellano and Dr. Radiy Islangulov for their assistance with fluorescence lifetime measurements.

REFERENCES

1. Weissleder R. *Nat. Biotechnol*. 2001; **19**: 316–317.
2. Weissleder R and Ntziachristos V. *Nat. Med*. 2003; **9**: 123–128.
3. Bremer C, Ntziachristos V and Weissleder R. *Eur. Radiol*. 2003; **13**: 231–243.
4. Frangioni JV. *Curr. Opin. Chem. Biol*. 2003; **7**: 626–634.
5. Hilderbrand SA and Weissleder R. *Curr. Opin. Chem. Biol*. 2010; **14**: 71–79.
6. Martínez-Díaz MV, de la Torre G and Torres T. *Chem. Commun*. 2010; **46**: 7090–7108.
7. Liu Y, Lin H, Dy JT, Tamaki K, Nakazaki J, Nakayama D, Uchida S, Kubo T and Segawa H. *Chem. Commun*. 2011; **47**: 4010–4012.
8. Chang Y-C, Wang C-L, Pan T-Y, Hong S-H, Lan C-M, Kuo H-H, Lo C-F, Hsu H-Y, Lin C-Y and Diau EW-G. *Chem. Commun*. 2011; **47**: 8910–8912.
9. Mathew S, Yella A, Gao P, Humphry-Baker R, Curchod BFE, Ashari-Astani N, Tavernelli I, Rothlisberger U, Nazeeruddin MK and Grätzel M. *Nature Chem*. 2014; **6**: 242–247.
10. D'Souza F, Amin AN, El-Khouly ME, Subbaiyan NK, Zandler ME and Fukuzumi S. *J. Am. Chem. Soc*. 2012; **134**: 654–664.
11. Balzani V, Credi A and Venturi M. *ChemSusChem* 2008; **1**: 26–58.
12. Roncali J. *Chem. Rev*. 1997; **97**: 173–205.
13. van Mullekom HAM, Vekemans JAJM, Havinga EE and Meijer EW. *Mater. Sci. Eng*. 2001; **32**: 1–40.
14. Tsuda A and Osuka A. *Science* 2001; **293**: 79–82.
15. Kiyose K, Kojima H and Nagano T. *Chem. Asian J*. 2008; **3**: 506–515.
16. Escobedo JO, Rusin O, Lim S and Strongin RM. *Curr. Opin. Chem. Biol*. 2010; **14**: 64–70.
17. Qian G and Wang ZY. *Chem. Asian J*. 2010; **5**: 1006–1029.
18. Luo S, Zhang E, Su Y, Cheng T and Shi C. *Biomaterials* 2011; **32**: 7127–7138.
19. Mori H, Tanaka T and Osuka A. *J. Mater. Chem. C* 2013; **1**: 2500–2519.
20. Zhao W and Carreira EM. *Angew. Chem. Int. Ed*. 2005; **44**: 1677–1679.
21. Umezawa K, Nakamura Y, Makino H, Citterio D and Suzuki K. *J. Am. Chem. Soc*. 2008; **130**: 1550–1551.

22. Strickler SJ and Berg RA. *J. Chem. Phys*. 1962; **37**: 814–822.
23. Englman R and Jortner J. *Mol. Phys*. 1970; **18**: 145–164.
24. Gouterman M. *J. Mol. Spectrosc*. 1961; **6**: 138–163.
25. Finikova OS, Cheprakov AV and Vinogradov SA. *J. Org. Chem*. 2005; **70**: 9562–9572.
26. Nakamura J, Okujima T, Tomimori Y, Komobuchi N, Yamada H, Uno H and Ono N. *Heterocycles* 2010; **80**: 1165–1175.
27. Davis NKS, Thompson AL and Anderson HL. *Org. Lett*. 2010; **12**: 2124–2127.
28. Davis NKS, Thompson AL and Anderson HL. *J. Am. Chem. Soc*. 2011; **133**: 30–31.
29. Diev VV, Schlenker CW, Hanson K, Zhong Q, Zimmerman JD, Forrest SR and Thompson ME. *J. Org. Chem*. 2012; **77**: 143–159.
30. Sauer K, Smith JRL and Schultz AJ. *J. Am. Chem. Soc*. 1966; **88**: 2681–2688.
31. Connolly JS, Samuel EB and Janzen AF. *Photochem. Photobiol*. 1982; **36**: 565–574.
32. Forster LS and Livingston R. *J. Chem. Phys*. 1952; **20**: 1315–1320.
33. Kee HL, Kirmaier C, Tang Q, Diers JR, Muthiah C, Taniguchi M, Laha JK, Ptaszek M, Lindsey JS, Bocian DF and Holten D. *Photochem. Photobiol*. 2007; **83**: 1110–1124.
34. Taniguchi M, Cramer DL, Bhise AD, Kee HL, Bocian DF, Holten D and Lindsey JS. *New J. Chem*. 2008; **32**: 947–958.
35. Kozyrev A, Ethirajan M, Chen P, Ohkubo K, Robinson BC, Barkigia KM, Fukuzumi S, Kadish KM and Pandey RK. *J. Org. Chem*. 2012; **77**: 10260–10271.
36. Seybold PG and Gouterman M. *J. Mol. Spectrosc*. 1969; **31**: 1–13.
37. Kobayashi N, Ogata H, Nonaka N and Luk'yanets EA. *Chem. Eur. J*. 2003; **9**: 5123–5134.
38. Susumu K, Maruyama H, Kobayashi H and Tanaka K. *J. Mater. Chem*. 2001; **11**: 2262–2270.
39. Lin VS-Y, DiMagno SG and Therien MJ. *Science* 1994; **264**: 1105–1111.
40. Lin VS-Y and Therien MJ. *Chem. Eur. J*. 1995; **1**: 645–651.
41. Angiolillo PJ, Lin VS-Y, Vanderkooi JM and Therien MJ. *J. Am. Chem. Soc*. 1995; **117**: 12514–12527.
42. LeCours SM, DiMagno SG and Therien MJ. *J. Am. Chem. Soc*. 1996; **118**: 11854–11864.
43. LeCours SM, Philips CM, de Paula JC and Therien MJ. *J. Am. Chem. Soc*. 1997; **119**: 12578–12589.
44. Kumble R, Palese S, Lin VS-Y, Therien MJ and Hochstrasser RM. *J. Am. Chem. Soc*. 1998; **120**: 11489–11498.
45. Shediac R, Gray MHB, Uyeda HT, Johnson RC, Hupp JT, Angiolillo PJ and Therien MJ. *J. Am. Chem. Soc*. 2000; **122**: 7017–7033.
46. Fletcher JT and Therien MJ. *J. Am. Chem. Soc*. 2000; **122**: 12393–12394.
47. Angiolillo PJ, Susumu K, Uyeda HT, Lin VS-Y, Shediac R and Therien MJ. *Synth. Met*. 2001; **116**: 247–253.
48. Fletcher JT and Therien MJ. *Inorg. Chem*. 2002; **41**: 331–341.
49. Fletcher JT and Therien MJ. *J. Am. Chem. Soc*. 2002; **124**: 4298–4311.
50. Susumu K and Therien MJ. *J. Am. Chem. Soc*. 2002; **124**: 8550–8552.
51. Rubtsov IV, Susumu K, Rubtsov GI and Therien MJ. *J. Am. Chem. Soc*. 2003; **125**: 2687–2696.
52. Redmore NP, Rubtsov IV and Therien MJ. *J. Am. Chem. Soc*. 2003; **125**: 8769–8778.
53. Rubtsov IV, Redmore NP, Hochstrasser RM and Therien MJ. *J. Am. Chem. Soc*. 2004; **126**: 2684–2685.
54. Angiolillo PJ, Uyeda HT, Duncan TV and Therien MJ. *J. Phys. Chem. B* 2004; **108**: 11893–11903.
55. Susumu K, Duncan TV and Therien MJ. *J. Am. Chem. Soc*. 2005; **127**: 5186–5195.
56. Susumu K, Frail PR, Angiolillo PJ and Therien MJ. *J. Am. Chem. Soc*. 2006; **128**: 8380–8381.
57. Duncan TV, Susumu K, Sinks LE and Therien MJ. *J. Am. Chem. Soc*. 2006; **128**: 9000–9001.
58. Duncan TV, Wu SP and Therien MJ. *J. Am. Chem. Soc*. 2006; **128**: 10423–10435.
59. Frail PR, Susumu K, Huynh M, Fong J, Kikkawa JM and Therien MJ. *Chem. Mater*. 2007; **19**: 6062–6064.
60. Duncan TV, Ishizuka T and Therien MJ. *J. Am. Chem. Soc*. 2007; **129**: 9691–9703.
61. Duncan TV, Frail PR, Miloradovic IR and Therien MJ. *J. Phys. Chem. B* 2010; **114**: 14696–14702.
62. Angiolillo PJ, Rawson J, Frail PR and Therien MJ. *Chem. Commun*. 2013; **49**: 9722–9724.
63. LeCours SM, Guan H-W, DiMagno SG, Wang CH and Therien MJ. *J. Am. Chem. Soc*. 1996; **118**: 1497–1503.
64. Priyadarshy S, Therien MJ and Beratan DN. *J. Am. Chem. Soc*. 1996; **118**: 1504–1510.
65. Karki L, Vance FW, Hupp JT, LeCours SM and Therien MJ. *J. Am. Chem. Soc*. 1998; **120**: 2606–2611.
66. Uyeda HT, Zhao Y, Wostyn K, Asselberghs I, Clays K, Persoons A and Therien MJ. *J. Am. Chem. Soc*. 2002; **124**: 13806–13813.
67. Duncan TV, Rubtsov IV, Uyeda HT and Therien MJ. *J. Am. Chem. Soc*. 2004; **126**: 9474–9475.
68. Zhang T-G, Zhao Y, Asselberghs I, Persoons A, Clays K and Therien MJ. *J. Am. Chem. Soc*. 2005; **127**: 9710–9720.
69. Zhang T-G, Zhao Y, Song K, Asselberghs I, Persoons A, Clays K and Therien MJ. *Inorg. Chem*. 2006; **45**: 9703–9712.
70. Xu T, Wu SP, Miloradovic I, Therien MJ and Blasie JK. *Nano Lett*. 2006; **6**: 2387–2394.
71. Duncan TV, Song K, Hung S-T, Miloradovic I, Nayak A, Persoons A, Verbiest T, Therien MJ and Clays K. *Angew. Chem. Int. Ed*. 2008; **47**: 2978–2981.

72. Keinan S, Therien MJ, Beratan DN and Yang W. *J. Phys. Chem. A* 2008; **112**: 12203–12207.
73. Therien MJ. *Nature* 2009; **458**: 716–717.
74. Hu X, Xiao D, Keinan S, Asselberghs I, Therien MJ, Clays K, Yang W and Beratan DN. *J. Phys. Chem. C* 2010; **114**: 2349–2359.
75. Gonella G, Dai H-L, Fry HC, Therien MJ, Krishnan V, Tronin A and Blasie JK. *J. Am. Chem. Soc*. 2010; **132**: 9693–9700.
76. Krishnan V, Tronin A, Strzalka J, Fry HC, Therien MJ and Blasie JK. *J. Am. Chem. Soc*. 2010; **132**: 11083–11092.
77. Singh-Rachford TN, Nayak A, Muro-Small ML, Goeb S, Therien MJ and Castellano FN. *J. Am. Chem. Soc*. 2010; **132**: 14203–14211.
78. Ishizuka T, Sinks LE, Song K, Hung S-T, Nayak A, Clays K and Therien MJ. *J. Am. Chem. Soc*. 2011; **133**: 2884–2896.
79. Jiang N, Zuber G, Keinan S, Nayak A, Yang W, Therien MJ and Beratan DN. *J. Phys. Chem. C* 2012; **116**: 9724–9733.
80. Fry HC, Lehmann A, Sinks LE, Asselberghs I, Tronin A, Krishnan V, Blasie JK, Clays K, DeGrado WF, Saven JG and Therien MJ. *J. Am. Chem. Soc*. 2013; **135**: 13914–13926.
81. Deria P, Bargen CDV, Olivier J-H, Kumbhar AS, Saven JG and Therien MJ. *J. Am. Chem. Soc*. 2013; **135**: 16220–16234.
82. Ostrowski JC, Susumu K, Robinson MR, Therien MJ and Bazan GC. *Adv. Mater*. 2003; **15**: 1296–1300.
83. Banerjee P, Conklin D, Nanayakkara S, Park T-H, Therien MJ and Bonnell DA. *ACS Nano* 2010; **4**: 1019–1025.
84. Conklin D, Park T-H, Nanayakkara S, Therien MJ and Bonnell DA. *Adv. Funct. Mater*. 2011; **21**: 4712–4718.
85. Conklin D, Nanayakkara S, Park T-H, Lagadec MF, Stecher JT, Therien MJ and Bonnell DA. *Nano Lett.* 2012; **12**: 2414–2419.
86. Li Z, Park T-H, Rawson J, Therien MJ and Borguet E. *Nano Lett*. 2012; **12**: 2722–2727.
87. Conklin D, Nanayakkara S, Park T-H, Lagadec MF, Stecher JT, Chen X, Therien MJ and Bonnell DA. *ACS Nano* 2013; **7**: 4479–4486.
88. Ghoroghchian PP, Frail PR, Susumu K, Blessington D, Brannan AK, Bates FS, Chance B, Hammer DA and Therien MJ. *Proc. Natl. Acad. Sci. USA* 2005; **102**: 2922–2927.
89. Ghoroghchian PP, Frail PR, Susumu K, Park T-H, Wu SP, Uyeda HT, Hammer DA and Therien MJ. *J. Am. Chem. Soc*. 2005; **127**: 15388–15390.
90. Wu SP, Lee I, Ghoroghchian PP, Frail PR, Zheng G, Glickson JD and Therien MJ. *Bioconjugate Chem*. 2005; **16**: 542–550.
91. Ghoroghchian PP, Lin JJ, Brannan AK, Frail PR, Bates FS, Therien MJ and Hammer DA. *Soft Matter* 2006; **2**: 973–980.
92. Ghoroghchian PP, Frail PR, Li G, Zupancich JA, Bates FS, Hammer DA and Therien MJ. *Chem. Mater*. 2007; **19**: 1309–1318.
93. Christian NA, Milone MC, Ranka SS, Li G, Frail PR, Davis KP, Bates FS, Therien MJ, Ghoroghchian PP, June CH and Hammer DA. *Bioconjugate Chem*. 2007; **18**: 31–40.
94. Duncan TV, Ghoroghchian PP, Rubtsov IV, Hammer DA and Therien MJ. *J. Am. Chem. Soc*. 2008; **130**: 9773–9784.
95. Ghoroghchian PP, Therien MJ and Hammer DA. *Wiley Interdiscip. Rev.: Nanomed. Nanobiotechnol*. 2009; **1**: 156–167.
96. Christian NA, Benencia F, Milone MC, Li G, Frail PR, Therien MJ, Coukos G and Hammer DA. *Mol. Imaging Biol*. 2009; **11**: 167–177.
97. Kamat NP, Liao Z, Moses LE, Rawson J, Therien MJ, Dmochowski IJ and Hammer DA. *Proc. Natl. Acad. Sci. U.S.A*. 2011; **108**: 13984–13989.
98. Pilgram K, Zupan M and Skiles R. *J. Heterocycl. Chem*. 1970; **7**: 629–633.
99. Susumu K, Fisher JAN, Zheng J, Beratan DN, Yodh AG and Therien MJ. *J. Phys. Chem. A* 2011; **115**: 5525–5539.
100. Quimby DJ and Longo FR. *J. Am. Chem. Soc*. 1975; **97**: 5111–5117.
101. Velusamy M, Justin Thomas KR, Lin JT, Hsu Y-C and Ho K-C. *Org. Lett*. 2005; **7**: 1899–1902.
102. Bundgaard E and Krebs FC. *Sol. Energy Mater. Sol. Cells* 2007; **91**: 954–985.
103. Linnanto J and Korppi-Tommola J. *J. Phys. Chem. A* 2001; **105**: 3855–3866.
104. Neto BAD, Lapis AAM, Júnior ENdS and Dupont J. *Eur. J. Org. Chem*. 2013: 228–255.